Equilibrium Sampling of Hard Spheres up to the Jamming Density and Beyond

Ludovic Berthier,[1] Daniele Coslovich,[1] Andrea Ninarello,[1] and Misaki Ozawa[1,2]

[1]*Laboratoire Charles Coulomb, UMR 5221 CNRS—Université de Montpellier, Montpellier 34095, France*
[2]*Department of Physics, Nagoya University, Nagoya 464-8602, Japan*

We implement and optimize a particle-swap Monte Carlo algorithm that allows us to thermalize a polydisperse system of hard spheres up to unprecedentedly large volume fractions, where previous algorithms and experiments fail to equilibrate. We show that no glass singularity intervenes before the jamming density, which we independently determine through two distinct nonequilibrium protocols. We demonstrate that equilibrium fluid and nonequilibrium jammed states can have the same density, showing that the jamming transition cannot be the end point of the fluid branch.

We clarify the behavior of noncrystalline states of hard spheres at very large densities where both a glass transition (in colloidal systems) and a jamming transition (in non-Brownian systems) are observed [1–3]. Glass and jamming transitions are usually studied through distinct protocols, and understanding the relation between these two broad classes of phase transformations and the resulting amorphous arrested states is an important research goal [1–5]. These questions impact a wide range of fields, from the rheological properties of soft materials to optimization problems in computer science [1,6].

Let us first consider Brownian hard spheres. When size polydispersity is introduced, crystallization can be prevented and the thermodynamic properties of the fluid studied at increasing density until a glass transition takes place, where particle diffusivity becomes very small [7]. Upon further compression, the pressure of the glass increases until a jamming transition occurs, where particles come at close contact and the pressure diverges [8]. Because the laboratory glass transition arises from using a finite observation time scale, two scenarios were proposed to describe the hypothetical situation where thermalization is no longer an issue [9]. A first possibility is that slower compressions reveal an ideal glass transition density, φ_0, above which the equilibrium state is a glass, not a fluid [2]. Jamming would then be observed upon further nonequilibrium compression of these glass states [10]. Alternatively, it may be that slower compressions continuously shift the kinetic glass transition to higher densities. In this view, it is plausible that jamming becomes the end point of the equilibrium fluid branch [11,12].

Distinguishing between these two scenarios by direct numerical measurements is challenging. For a well-studied binary mixture of hard spheres, for instance, thermalization can be achieved up to $\varphi_{max} \approx 0.60$ [9,13]. The location of the glass transition must be extrapolated using empirical fits based on activated relaxation. Values in the range $\varphi_0 = 0.615$–0.635 were obtained [9], depending on the fitting function. Fitting the relaxation times to a power law yields

$\varphi_{mct} \approx 0.59 < \varphi_{max}$, so that the associated mode-coupling transition [14] corresponds to an avoided singularity. For the same system, jamming transitions were located in the range $\varphi_J = 0.648$–0.662 depending on the chosen protocol [15–17]. The relation between glass and jamming transitions is left unresolved, as thermalization stops long before any of the singularities can be crossed, $\varphi_{max} \ll \varphi_0$, φ_J, and because estimates of φ_0 and φ_J are too close to favor any of the above scenarios. Similar inconclusive results are obtained for polydisperse hard spheres with a continuous particle size distribution; see Fig. 1. Our standard Monte Carlo simulations yield slightly different values for the various critical densities, but they again fall out of
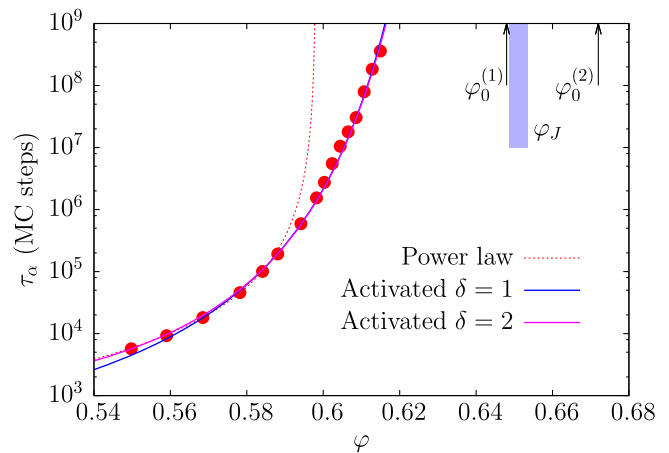

FIG. 1. Equilibrium relaxation time scale of polydisperse ($\Delta = 23\%$) hard spheres from conventional Monte Carlo simulations. The power law fit provides an estimate of the location of the avoided mode-coupling transition, $\varphi_{mct} \approx 0.598$; activated relaxation fits, $\exp[B/(\varphi_0 - \varphi)^\delta]$, yield possible locations for the extrapolation of a diverging time scale, $\varphi_0^{(1)} \approx 0.648$, when $\delta = 1$ and $\varphi_0^{(2)} \approx 0.672$ for $\delta = 2$. The range of jamming densities $0.6487 < \varphi_J < 0.6534$ using nonequilibrium protocols (the shaded area) overlaps with the range of the extrapolated dynamical divergences.

equilibrium too early to disentangle glass and jamming transitions.

Our main achievement is the numerical proof that firm conclusions on these questions can be drawn by implementing a more efficient Monte Carlo sampling method. The key enabling factor of our computational approach is the combination of swap Monte Carlo moves and standard single-particle translations [18–20], which is a simple instance of a cluster move [21,22]. Swap moves enhance thermalization in simple mixtures [23], but their efficiency is significantly higher in continuously polydisperse systems [24–26]. We show that this optimized sampling method allows us to thermalize polydisperse hard spheres up to unprecedentedly large densities. In particular, we achieve thermal equilibrium in a region of densities where the jamming transition φ_J can also be located by accepted methods [9,15,27]. This directly shows, without extrapolating any dynamical data, that point J of jamming does not correspond to the end point of the fluid equilibrium states. Our results also imply that the ideal glass transition, if it exists, occurs in our system at an even larger density, $\varphi_0 > \varphi_J$. Conceptually, our results demonstrate that jamming and glass transitions explore distinct parts of the configuration space, far from and close to equilibrium, respectively.

We study the canonical model of hard spheres in three dimensions. The pair interaction is zero for nonoverlapping particles, infinite otherwise. We use a continuous size polydispersity, where the particle diameter is distributed according to $p(\sigma_m \leq \sigma \leq \sigma_M) = A/\sigma^3$, where A is a normalization constant. Because of our enhanced Monte Carlo sampling (see below), crystallization, which does not occur for ordinarily studied size polydispersities, $\Delta = \sqrt{\overline{\sigma^2} - \overline{\sigma}^2}/\overline{\sigma} \sim 8\%-14\%$, and standard Monte Carlo dynamics, is easily observed in our simulations. Therefore, to more deeply penetrate the relevant glassy region and avoid crystal formation [28], we use a larger polydispersity of $\Delta = 23\%$, choosing $\sigma_m/\sigma_M = 0.4492$. We simulate systems composed of $N = 300$, 1000, and 8000 particles in a cubic cell with periodic boundary conditions. We present mainly data for $N = 1000$, except where otherwise specified. Dynamical relaxation is recorded by measuring the self-intermediate scattering function $F_s(k, t)$ at a wave number k corresponding to the first maximum of the structure factor. In constant volume simulations, we measure the pressure P using the contact value of the pair correlation function [29]. We also perform constant pressure simulations where φ fluctuates [30,31]. The reduced pressure is $Z = P/(\rho k_B T)$, where ρ is the number density and $k_B T$ is the thermal energy. Times are reported using standard Monte Carlo time steps [32].

Starting with conventional Monte Carlo dynamics with translational moves drawn over a cube of linear size $0.115\overline{\sigma}$, we measure the equilibrium relaxation time τ_α of the system from the time decay of the self-intermediate
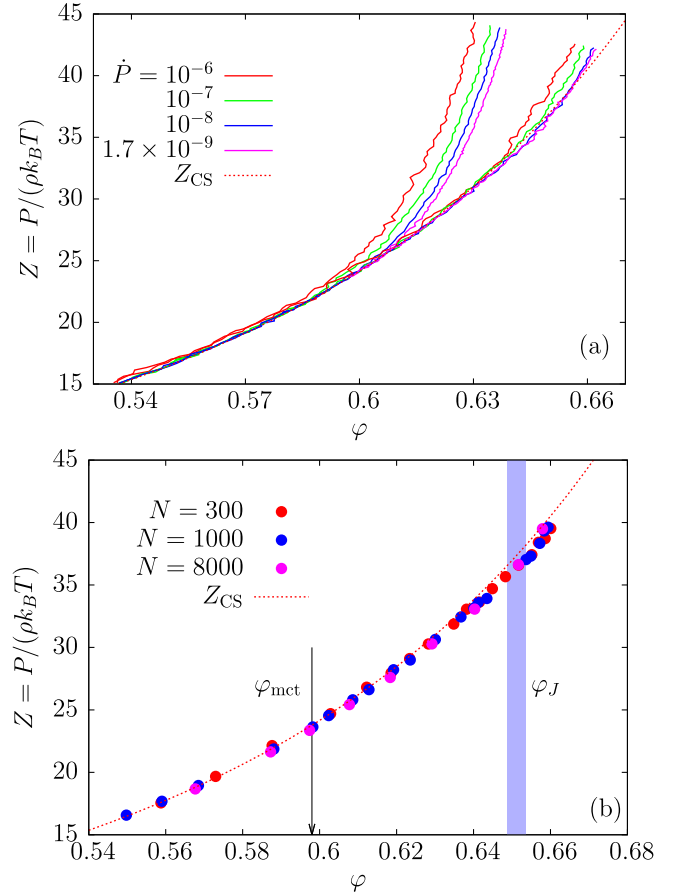

FIG. 2. (a) Reduced pressure Z during compressions at finite rates $\dot{P}$ with (right curves) and without (left curves) swap. The swap Monte Carlo method falls out of equilibrium at much larger volume fractions than conventional sampling. (b) Equilibrium measurements of the equation of state (the symbols) for different system sizes. Our equilibrium data go beyond the shaded area, which represents the determined range of jamming densities. In both panels, the dashed line is the Carnahan-Stirling empirical expression [33,34].

scattering function, $F_s(k, \tau_\alpha) = 1/e$; see Fig. 1. We observe an appreciable growth of about 5 orders of magnitude and we can use standard functional forms to locate several characteristic densities for viscous slowdown. First, we locate the mode-coupling crossover using a power law, $\tau_\alpha \sim (\varphi_{\mathrm{mct}} - \varphi)^{-\gamma}$. We get $\varphi_{\mathrm{mct}} \approx 0.598$. As shown in Fig. 1, we can thermalize the system beyond φ_{mct} and conclude that this singularity is avoided [13,21]. We then use an activated relaxation fit, $\tau_\alpha \sim \exp[B/(\varphi_0 - \varphi)^\delta]$, to extrapolate the location of the diverging relaxation time. We get $\varphi_0^{(1)} \approx 0.648$ for $\delta = 1$ and $\varphi_0^{(2)} \approx 0.672$, using the exponent $\delta = 2$ favored in earlier studies [9,13]. The resulting range of φ_0 proves that extrapolating φ_0 from conventional simulations is a difficult exercise.

When $\varphi > \varphi_{\max} \approx 0.605$, standard Monte Carlo simulations fall out of equilibrium. This is proved in Fig. 2(a), where we report the evolution of $Z = Z(\varphi)$ in simulations

where we slowly increase the pressure at a finite rate $\dot{P}$ varying from $\dot{P} = 10^{-6}$ down to 1.7×10^{-9}. Changing $\dot{P}$ over nearly 4 orders of magnitude shows that thermalization is achieved up to increasingly large densities, but φ_{max} increases slowly with a decreasing $\dot{P}$, with clear deviations from the fluid equation of state when $\varphi > \varphi_{max}$.

We now boost thermalization by implementing a swap algorithm [18–20]. With probability α, we perform conventional Monte Carlo moves where particles are translated, and with probability $(1 - \alpha)$ we perform a swap move where we pick two particles at random and attempt to exchange their diameters. The swap is accepted if it does not create an overlap. By measuring the structural relaxation times with swap Monte Carlo dynamics, we find that $\alpha \approx 0.80$ is the optimal value for fast thermalization [26], with an efficiency that, remarkably, does not depend on system size.

This algorithm respects detailed balance and thus provides a correct sampling of phase space. That it also dramatically enhances the sampling efficiency is demonstrated in Fig. 2(a), where we compress the system using the same compression rates $\dot{P}$ as before, but now by combining swap and translational moves. Whereas the new sampling method again falls out of equilibrium at large enough densities, we observe that for $\varphi < \varphi_{max}^{swap} \approx 0.655$, $Z(\varphi)$ does not depend on $\dot{P}$. The increase of φ_{max} from 0.605 to 0.655 is significant, as $\dot{P}$ should be slower by many orders of magnitude for the standard dynamics to perform as well as the swap method. The system shows no tendency to crystalline order, which would appear as a horizontal liquid-crystal coexistence plateau in Fig. 2(a). We further checked the absence of crystalline order for $\Delta = 23\%$ using standard bond-orientational order analysis [35] and analysis of locally favored structures [36]. We also checked to see that fractionation and size segregation do not occur by observing partial structure factors for higher and smaller particles. By contrast, we observed crystallization at large φ for lower values of Δ. Thus, we conclude from Fig. 2(a) that our model is both robust against crystallization and easy to thermalize at extremely large densities using optimized swap Monte Carlo dynamics. This represents a major methological progress for computer simulations of glassy materials.

We now perform equilibrium measurements of the pressure for each density where thermalization can be achieved. By carefully checking that aging is absent in fully relaxing time correlation functions (particularly density correlations) in long simulation runs of up to 10^{10} swap Monte Carlo steps, we confirmed that thermalization is achieved for all N's up to $\varphi_{max}^{swap} \approx 0.655$, directly establishing that no ergodicity breaking occurs below this point. Equilibrium results for the equation of state $Z(\varphi)$ are reported in Fig. 2(b) for various system sizes. We find that the empirical Carnahan-Starling (CS) equation of state for polydisperse hard spheres [33,34], Z_{CS}, describes our numerical data surprisingly well up to the largest studied density. Closer

inspection reveals that small deviations from Z_{CS} appear near $\varphi \approx 0.63$, above which $Z < Z_{CS}$. Earlier reports had instead found opposite deviations from the CS equation of state [8,37–39], probably due to insufficient thermalization, as we also observe when using finite compression rates. Also, we do not find evidence for a singular density describing the equilibrium equation of state.

From these equilibrium data, it is clear that the extrapolated singularity at $\varphi_0^{(1)} = 0.648$ (Fig. 1) is not observed, which shows that the activated relaxation fit with $\delta = 1$, akin to the Vogel-Fulcher-Tamman law for molecular glasses [40], must break down between $\varphi_{max} = 0.605$ and $\varphi_0^{(1)} = 0.648$. An ideal glass transition, if present, must occur above $\varphi_{max}^{swap} = 0.655$. Therefore, our second extrapolated value, $\varphi_0^{(2)} = 0.672$, is not ruled out.

We now determine the location of the point J of jamming for our system. Following earlier works, we employed two distinct numerical protocols. In a first approach, we perform very rapid compressions of dilute hard sphere fluid configurations using Monte Carlo simulations without swap [9]. We impose a very large pressure, $P = 10^6$, and measure the longtime limit of the volume fraction. These fast compressions yield $\varphi_J^{(1)} \approx 0.6487$. In an independent protocol, we use energy minimization procedures converting the hard sphere potential into soft harmonic repulsive springs [15,27], which defines "point J" [15]. We iteratively compress or expand the system starting from a dilute random system distribution until particles are precisely at contact [27]. We obtain $\varphi_J^{(2)} \approx 0.6534$. These two values are compatible with earlier determinations of the jamming transition for polydisperse systems [41]. Note that slower protocols would jam at larger packing fractions [16]. While jammed configurations produced by the energy minimization protocol are always isostatic, those obtained using very rapid Monte Carlo compressions are slightly hypostatic [42]. This might explain the small difference between $\varphi_J^{(1)}$ and $\varphi_J^{(2)}$ [16].

In Fig. 2(b), we show that the equilibrium equation of state of the fluid can be measured up to φ_J *and beyond*, demonstrating that φ_J cannot be the end point of the fluid branch. These data indicate, therefore, that φ_0, if it exists, must actually be larger than φ_J. If the jamming transition does not control the large-pressure behavior of the equilibrium fluid, its potential connection to glassy dynamics is then considerably weakened. Fundamentally, the decoupling between glass and jamming exposed by our measurements occurs because jamming is observed using protocols that are very far from thermal equilibrium. Instead, in the presence of thermal fluctuations, the configurational space is sampled with the Boltzmann probability distribution. Distinct sets of configurations are thus explored in thermal and athermal protocols.

Both to confirm this fundamental difference and to reinforce our conclusion that fluid and jammed states
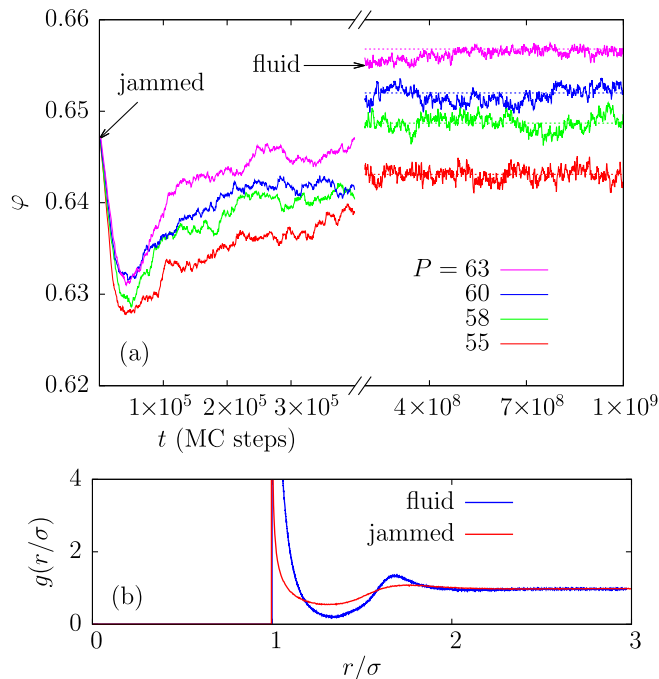
FIG. 3.   (a) Memory effect in hard spheres. Time evolution of the volume fraction starting at $t = 0$ from a jammed configuration in constant pressure swap Monte Carlo simulations. A nonmonotonic evolution of the density is observed, showing that jammed and fluid states are structurally distinct. At long times (note the break in the time axis), steady state fluctuations are observed both below and above φ_J around the value (dashed lines) obtained from the equation of state. (b) Pair distribution functions of rescaled distances $r_{ij}/[(\sigma_i + \sigma_j)/2]$ are distinct for fluid and jammed states near $\varphi = 0.6534$.

may exist over a similar density range, we perform the memory experiment shown in Fig. 3(a). We start simulations using the nearly jammed configurations created by fast Monte Carlo compressions of dilute fluid states. The pressure in these states is very large, $P = 10^6$. At time $t = 0$, we start a constant pressure Monte Carlo simulation involving particle swaps, for a range of pressures P chosen such that the corresponding equilibrium volume fractions lie in the vicinity of φ_J. Therefore, at the time $t = 0^+$, the volume fraction has a value which is already very close to its equilibrium value. If jammed and fluid states were to be structurally close to one another, the density should exhibit a mild time dependence, having similar values at small and large times. The results in Fig. 3(a) instead demonstrate a more complex time dependence with a pronounced nonmonotonic behavior. Readers familiar with the physics of disordered materials will recognize this protocol as a memory (or Kovacs) effect [43]. Similar nonmonotonic behaviors were observed in a variety of glassy systems, from polymer glasses to granular media and spin glasses [40,44–48].

As soon as the pressure is set to a finite value, the system undergoes a rapid expansion from the jammed initial

configuration, accompanied by little particle diffusion. Under the influence of the swap Monte Carlo dynamics, particles diffuse and the system starts to thermally explore fluid configurations in order to reach equilibrium at long times. During this aging process, the volume fraction slowly increases, which explains the nonmonotonic time dependence. At very large times, the density reaches its steady state equilibrium value, which depends on the applied pressure through the equilibrium equation of state. The time series in Fig. 3 indicate that stationary fluid states exist below, at, and above φ_J, whereas the nonmonotonic time dependence of the volume fraction demonstrates that typical jammed and high density fluid configurations are structurally very distinct, as testified by the pair correlation functions shown in Fig. 3(b). The structure of fluid and jammed states differs not only near contact [where the jammed $g(r)$ is highly singular] but also farther away from contact.

In conclusion, we presented numerical measurements of the fluid equation of state of hard spheres in a part of the phase diagram that has thus far been unaccessible to both numerical simulations and experiments. Our results rule out the possibility that the jamming transition represents the end point of the fluid equation of state [11,12], and they suggest that a glass transition, if it exists, is logically disconnected from the jamming transition. This situation contrasts with both leading scenarios discussed in the Introduction, although it fits naturally in theories where jamming densities span a finite range of protocol-dependent values [2,10]. A similar scenario is found in quasi-one-dimensional channels, where equilibrium fluid and jammed states also coexist over a density range [49].

The efficiency of the optimized Monte Carlo sampling developed here, combined with a sufficient degree of particle size polydispersity [50], paves the way for a set of novel studies of glassy states in amorphous materials. We expect this approach to be fruitful in elucidating a number of outstanding aspects of the glass problem, such as the existence of the Gardner transition in finite dimensional systems [51,52], the growth of static point-to-set correlations [53–55] and locally favored structures [56], measurements of configurational entropy [57], and the physics of ultrastable glasses [58].

[1] A. J. Liu and S. R. Nagel, Nature (London) **396**, 21 (1998).
[2] G. Parisi and F. Zamponi, Rev. Mod. Phys. **82**, 789 (2010).
[3] L. Berthier, G. Biroli, J.-P. Bouchaud, L. Cipelletti, and W. v. Saarloos, *Dynamical Heterogeneities in Glasses,*

Colloids, and Granular Media (Oxford University Press, New York, 2011).

[4] M. Pica Ciamarra, M. Nicodemi, and A. Coniglio, Soft Matter **6**, 2871 (2010).

[5] A. Ikeda, L. Berthier, and P. Sollich, Phys. Rev. Lett. **109**, 018301 (2012).

[6] M. Mézard and A. Montanari, *Information, Physics, and Computation* (Oxford University Press, Oxford, 2009).

[7] P. N. Pusey and W. van Megen, Phys. Rev. Lett. **59**, 2083 (1987).

[8] M. D. Rintoul and S. Torquato, Phys. Rev. Lett. **77**, 4198 (1996).

[9] L. Berthier and T. A. Witten, Phys. Rev. E **80**, 021502 (2009).

[10] R. Mari, F. Krzakala, and J. Kurchan, Phys. Rev. Lett. **103**, 025701 (2009).

[11] T. Aste and A. Coniglio, Europhys. Lett. **67**, 165 (2004).

[12] R. D. Kamien and A. J. Liu, Phys. Rev. Lett. **99**, 155501 (2007).

[13] G. Brambilla, D. El Masri, M. Pierno, L. Berthier, L. Cipelletti, G. Petekidis, and A. B. Schofield, Phys. Rev. Lett. **102**, 085703 (2009).

[14] W. Götze, *Complex Dynamics of Glass-Forming Liquids: A Mode-Coupling Theory* (Oxford University Press, New York, 2009).

[15] C. S. O'Hern, S. A. Langer, A. J. Liu, and S. R. Nagel, Phys. Rev. Lett. **88**, 075507 (2002).

[16] P. Chaudhuri, L. Berthier, and S. Sastry, Phys. Rev. Lett. **104**, 165701 (2010).

[17] M. Ozawa, T. Kuroiwa, A. Ikeda, and K. Miyazaki, Phys. Rev. Lett. **109**, 205701 (2012).

[18] D. Gazzillo and G. Pastore, Chem. Phys. Lett. **159**, 388 (1989).

[19] S. Pronk and D. Frenkel, Phys. Rev. E **69**, 066123 (2004).

[20] T. S. Grigera and G. Parisi, Phys. Rev. E **63**, 045102 (2001).

[21] L. Santen and W. Krauth, Nature (London) **405**, 550 (2000).

[22] E. P. Bernard and W. Krauth, Phys. Rev. Lett. **107**, 155704 (2011).

[23] R. Gutiérrez, S. Karmakar, Y. G. Pollack, and I. Procaccia, Europhys. Lett. **111**, 56009 (2015).

[24] Y. Brumer and D. Reichman, J. Phys. Chem. B **108**, 6832 (2004).

[25] L. A. Fernández, V. Martín-Mayor, and P. Verrocchio, Phys. Rev. Lett. **98**, 085702 (2007).

[26] A. Ninarello, L. Berthier, and D. Coslovich (to be published).

[27] N. Xu, J. Blawzdziewicz, and C. S. O'Hern, Phys. Rev. E **71**, 061306 (2005).

[28] L. A. Fernandez, V. Martin-Mayor, B. Seoane, and P. Verrocchio, Phys. Rev. E **82**, 021501 (2010).

[29] A. Santos, S. B. Yuste, and M. López de Haro, J. Chem. Phys. **123**, 234512 (2005).

[30] D. Frenkel and B. Smit, *Understanding Molecular Simulation*, 2nd ed. (Academic, New York, 2001).

[31] To adjust the pressure, we attempt compression-decompression moves at an average frequency of one box move every N translational particle moves. The typical attempted changes in the linear size of the box are at about 3%.

[32] L. Berthier and W. Kob, J. Phys. Condens. Matter **19**, 205130 (2007).

[33] T. Boublik, J. Chem. Phys. **53**, 471 (1970).

[34] G. A. Mansoori, N. F. Carnahan, K. E. Starling, and T. W. Leland, Jr., J. Chem. Phys. **54**, 1523 (1971).

[35] P. J. Steinhardt, D. R. Nelson, and M. Ronchetti, Phys. Rev. B **28**, 784 (1983).

[36] D. Coslovich and G. Pastore, J. Chem. Phys. **127**, 124504 (2007).

[37] M. Hermes and M. Dijkstra, J. Phys. Condens. Matter **22**, 104114 (2010).

[38] M. Hermes and M. Dijkstra, Europhys. Lett. **89**, 38005 (2010).

[39] G. Odriozola and L. Berthier, J. Chem. Phys. **134**, 054504 (2011).

[40] C. A. Angell, K. L. Ngai, G. B. McKenna, P. F. McMillan, and S. W. Martin, J. Appl. Phys. **88**, 3113 (2000).

[41] K. W. Desmond and E. R. Weeks, Phys. Rev. E **90**, 022204 (2014).

[42] A. Donev, S. Torquato, and F. H. Stillinger, Phys. Rev. E **71**, 011105 (2005).

[43] A. J. Kovacs, Adv. Polym. Sci **3/3**, 394 (1964).

[44] R. L. Leheny and S. R. Nagel, Phys. Rev. B **57**, 5154 (1998).

[45] F. Alberici-Kious, J.-P. Bouchaud, L. F. Cugliandolo, P. Doussineau, and A. Levelut, Phys. Rev. Lett. **81**, 4987 (1998).

[46] C. Josserand, A. Tkachenko, D. M. Mueth, and H. M. Jaeger, Phys. Rev. Lett. **85**, 3632 (2000).

[47] L. Berthier and J.-P. Bouchaud, Phys. Rev. B **66**, 054404 (2002).

[48] S. Mossa and F. Sciortino, Phys. Rev. Lett. **92**, 045504 (2004).

[49] M. Z. Yamchi, S. S. Ashwin, and R. K. Bowles, Phys. Rev. E **91**, 022301 (2015).

[50] Whereas our main conclusion about the interrelation between glass and jamming transitions should hold generally for an arbitrary particle size distribution, continuous or discrete, the possibility of developing an efficient swap Monte Carlo dynamics allowing the exploration of phase space at large density will depend on the chosen distribution [26].

[51] P. Charbonneau, J. Kurchan, G. Parisi, P. Urbani, and F. Zamponi, Nat. Commun. **5**, 3725 (2014).

[52] L. Berthier, P. Charbonneau, Y. Jin, G. Parisi, B. Seoane, and F. Zamponi, arXiv:1511.04201 [Proc. Natl. Acad. Sci. U.S.A. (to be published)].

[53] G. Biroli, J.-P. Bouchaud, A. Cavagna, T. Grigera, and P. Verrocchio, Nat. Phys. **4**, 771 (2008).

[54] G. M. Hocky, T. E. Markland, and D. R. Reichman, Phys. Rev. Lett. **108**, 225506 (2012).

[55] L. Berthier, P. Charbonneau, and S. Yaida, J. Chem. Phys. **144**, 024501 (2016).

[56] C. P. Royall and S. R. Williams, Phys. Rep. **560**, 1 (2015).

[57] L. Berthier and D. Coslovich, Proc. Natl. Acad. Sci. U.S.A. **111**, 11668 (2014).

[58] S. F. Swallen, K. L. Kearns, M. K. Mapes, Y. S. Kim, R. J. McMahon, M. D. Ediger, T. Wu, L. Yu, and S. Satija, Science **315**, 353 (2007).